

DUELING NETWORK ARCHITECTURES FOR DEEP REINFORCEMENT LEARNING

Ziyu Wang, Nando de Freitas & Marc Lanctot

Google DeepMind

London, UK

{ziyu,nandodefrees,lanctot}@google.com

ABSTRACT

In recent years there have been many successes of using deep representations in reinforcement learning. Still, many of these applications use conventional architectures, such as convolutional networks, LSTMs, or auto-encoders. In this paper, we present a new neural network architecture for model-free reinforcement learning inspired by advantage learning. Our dueling architecture represents two separate estimators: one for the state value function and one for the state-dependent action advantage function. The main benefit of this factoring is to generalize learning across actions without imposing any change to the underlying reinforcement learning algorithm. Our results show that this architecture leads to better policy evaluation in the presence of many similar-valued actions. Moreover, the dueling architecture enables our RL agent to outperform the state-of-the-art Double DQN method of van Hasselt et al. (2015) in 46 out of 57 Atari games.

1 INTRODUCTION

Over the past years, deep learning has contributed to dramatic advances in scalability and performance of machine learning (LeCun et al., 2015). One exciting application is the sequential decision-making setting of reinforcement learning (RL) and control. Notable examples include deep Q-learning (Mnih et al., 2015), deep visuomotor policies (Levine et al., 2015), attention with recurrent networks (Ba et al., 2015), and model predictive control with embeddings (Watter et al., 2015). Other recent successes include massively parallel frameworks (Nair et al., 2015) and expert move prediction in the game of Go (Maddison et al., 2015), which have produced policies matching those of Monte Carlo tree search programs.

In spite of this, most of the approaches for RL use standard neural networks, such as convolutional networks, MLPs, LSTMs and autoencoders. The focus in these recent advances has been on designing improved control and RL algorithms, or simply on incorporating existing neural network architectures into RL methods. Here, we take an *alternative but complementary approach* of focusing primarily on innovating a neural network architecture that is better suited for model-free RL. This approach has the benefit that the new network can be easily combined with existing and future algorithms for RL. That is, this paper advances a new network (Figure 1), but uses already published algorithms.

We propose a new network architecture, which we name the *dueling architecture*, that explicitly separates the representation of state values and (state-dependent) action advantages. The dueling architecture consists of two streams, sharing a common convolutional feature learning module, which represent the value and advantage functions. The two streams are combined via a special aggregating layer to produce an estimate of the state-action value function Q as shown in Figure 1. This dueling network should be understood as a single Q network that replaces the popular convolutional Q network in existing algorithms such as DQN (Mnih et al., 2015). The dueling network automatically produces separate estimates of the state value function and advan-

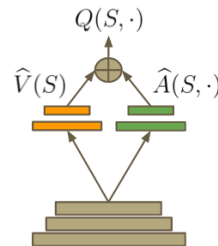


Figure 1: The dueling net.

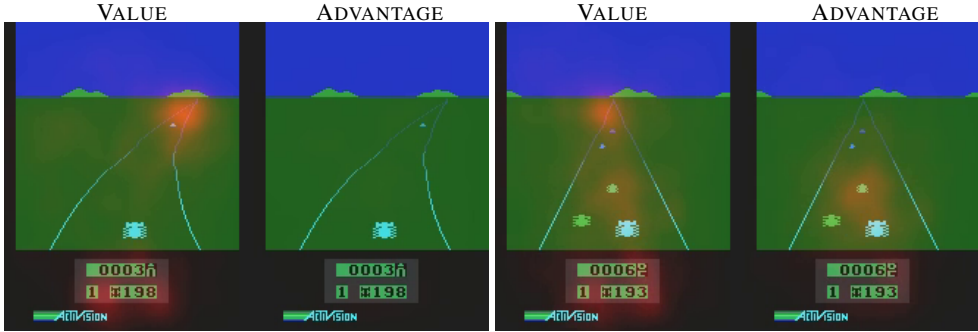


Figure 2: See, attend and drive: Value and advantage saliency maps on the Enduro game for a trained dueling architecture. The value stream learns to pay attention to the road. The advantage stream learns to pay attention only when there are cars immediately in front, so as to avoid collisions.

tage function, without any extra supervision. The new special aggregator that makes this possible is described in Section 3.

Intuitively, the dueling architecture can learn which states are (or are not) valuable, without having to learn the effect of each action for each state. This is particularly useful when the agent encounters itself in states where its actions do not affect the environment in any relevant way. To illustrate this, consider the saliency maps shown in Figure 2¹. These maps were generated by computing the Jacobians of the trained value and advantage streams with respect to the input video, following the method proposed by Simonyan et al. (2013). (The experimental section describes this methodology in more detail.) The figure shows the value and advantage saliency maps for two different time steps. In one time step (leftmost pair of images), we see that the value network stream pays attention to the road and in particular to the horizon, where new cars appear. It also pays attention to the score. The advantage stream on the other hand does not pay much attention to the visual input because its action choice is practically irrelevant when there are no cars in front. However, in the second time step (rightmost pair of images) the advantage stream pays attention as there is a car immediately in front, making its choice of action very relevant.

In the experiments, we demonstrate that the dueling architecture can more quickly identify the correct action during policy evaluation as redundant or similar actions are added to the learning problem. We also evaluate the gains brought in by the dueling architecture on the challenging Atari 2600 testbed. Here, an RL agent with the same structure and hyper-parameters must be able to play 57 different games by observing image pixels and game scores only. We show that our approach outperforms the baseline Deep Q-Networks (DQN) of Mnih et al. (2015) on 50 out of 57 games and the state-of-the-art Double DQN of van Hasselt et al. (2015)) on 46 out of 57 games.

On some games, such as Seaquest, replacing the convolutional Q-network with the dueling Q-network results in dramatic score improvements. For instance, under the 30 no-op actions performance measure, the scores for DQN, double DQN with a convolutional network, double DQN with the dueling network, and our best known human player are 5861, 16453, 50254 and 42055 respectively. The dueling network has enabled us to match human performance in this complex game.

1.1 RELATED WORK

The notion of maintaining separate value and advantage functions goes back to Baird (1993). In Baird’s original advantage updating algorithm, the shared Bellman residual update equation is decomposed into two updates: one for a state value function, and one for its associated advantage function. Advantage updating was shown to converge faster than Q-learning in simple continuous time domains in (Harmon et al., 1995). Its successor, the advantage learning algorithm, represents only a single advantage function (Harmon & Baird, 1996).

¹The saliency videos are available at <https://www.youtube.com/watch?v=TPGuQaswaHs&list=PLkmHIkh1FjiS2EGp3QNITDbA08MIYzupP>.

The dueling architecture represents both the value $V^\pi(s)$ and advantage $A^\pi(s, a)$ functions with a single deep model whose output combines the two to produce a state-action value $Q(s, a)$. Unlike in advantage updating, the representation and algorithm are decoupled by construction. Consequently, the dueling architecture can be used in combination with a myriad of model free RL algorithms.

There is a long history of advantage functions in policy gradients, starting with Sutton et al. (2000). As a recent example of this line of work, Schulman et al. (2015) estimate advantage values online to reduce the variance of policy gradient algorithms.

There have been several attempts at playing Atari with deep reinforcement learning, including Mnih et al. (2015); Guo et al. (2014); Stadie et al. (2015); Nair et al. (2015) and van Hasselt et al. (2015). The results of van Hasselt et al. (2015) are the current published state-of-the-art.

Simultaneously with our work, innovations in prioritized memory replay (see the co-submission by Schaul et al. (2015)) and in increasing the action gap (Bellemare et al., 2016) have also outperformed the state-of-the-art (van Hasselt et al., 2015). The improvements brought in by the prioritized replay and the dueling architecture are particularly dramatic. The two approaches have great merit on their own, while pursuing two very different but complementary research directions. Combining our dueling architecture with prioritized replay should lead to further improvements in the state-of-the-art.

2 BACKGROUND

We consider a sequential decision making setup, in which an agent interacts with an environment \mathcal{E} over discrete time steps, see Sutton & Barto (1998) for an introduction. In the Atari domain, for example, the agent perceives a video s_t consisting of M image frames: $s_t = (x_{t-M+1}, \dots, x_t) \in \mathcal{S}$ at time step t . The agent then chooses an action from a discrete set $a_t \in \mathcal{A} = \{1, \dots, |\mathcal{A}|\}$ and observes a reward signal r_t produced by the game emulator.

The agent seeks maximize the expected discounted return, where we define the discounted return as $R_t = \sum_{\tau=t}^{\infty} \gamma^{\tau-t} r_\tau$. In this formulation, $\gamma \in [0, 1]$ is a discount factor that trades-off the importance of immediate and future rewards.

For an agent behaving according to a stochastic policy π , the values of the state-action pair (s, a) and the state s are defined as follows

$$Q^\pi(s, a) = \mathbb{E}[R_t | s_t = s, a_t = a, \pi], \quad \text{and} \quad V^\pi(s) = \mathbb{E}_{a \sim \pi(s)}[Q^\pi(s, a)]. \quad (1)$$

The preceding state-action value function (Q function for short) can be computed recursively with dynamic programming:

$$Q^\pi(s, a) = \mathbb{E}_{s'}[r + \gamma \mathbb{E}_{a' \sim \pi(s')} [Q^\pi(s', a')] | s, a, \pi]. \quad (2)$$

The optimal Q function is defined as $Q^*(s, a) = \max_\pi Q^\pi(s, a)$. Under the deterministic policy $a = \arg \max_{a' \in \mathcal{A}} Q^*(s, a')$, it follows that $V^*(s) = \max_a Q^*(s, a)$. From this, it also follows that the optimal Q function satisfies the Bellman equation:

$$Q^*(s, a) = \mathbb{E}_{s'}[r + \gamma \max_{a'} Q^*(s', a') | s, a]. \quad (3)$$

We define another important quantity, the *advantage function*, relating the value and Q functions:

$$A^\pi(s, a) = Q^\pi(s, a) - V^\pi(s). \quad (4)$$

Note that $\mathbb{E}_{a \sim \pi(s)} [A^\pi(s, a)] = 0$. Intuitively, the value function V measures the importance of being in a particular state s . The Q function, however, measures the importance about the value of choosing each possible action when in this state. The advantage function subtracts the value of the state from the Q function to obtain a relative measure of the importance of each action.

2.1 DEEP Q-NETWORKS

The value functions as described in the preceding section are high dimensional objects. To approximate them, we can use a deep Q -network: $Q(s, a; \theta)$ with parameters θ . To estimate this network,

we optimize the following sequence of loss functions at iteration i :

$$L_i(\theta_i) = \mathbb{E}_{s,a,r,s'} \left[\left(y_i^{DQN} - Q(s, a; \theta_i) \right)^2 \right], \quad (5)$$

with

$$y_i^{DQN} = r + \gamma \max_{a'} Q(s', a'; \theta^-), \quad (6)$$

where θ^- represents the parameters of a fixed and separate *target network*. We could attempt to use standard Q -learning to learn the parameters of the network $Q(s, a; \theta)$ online. However, this estimator performs poorly in practice. A key innovation in (Mnih et al., 2015) was to freeze the parameters of the target network $Q(s', a'; \theta^-)$ for a fixed number of iterations while updating the *online network* $Q(s, a; \theta_i)$ by gradient descent. (This greatly improves the stability of the algorithm.) The specific gradient update is

$$\nabla_{\theta_i} L_i(\theta_i) = \mathbb{E}_{s,a,r,s'} \left[\left(r + \gamma \max_{a'} Q(s', a'; \theta^-) - Q(s, a; \theta_i) \right) \nabla_{\theta_i} Q(s, a; \theta_i) \right] \quad (7)$$

This approach is model free in the sense that the states and rewards are produced by the environment. It is also off-policy because these states and rewards are obtained with an behavior policy (epsilon greedy in DQN) different from the online policy that is being learned.

Another key ingredient behind the success of DQN is *experience replay* (Lin, 1993; Mnih et al., 2015). During learning, the agent accumulates a dataset $\mathcal{D}_t = \{e_1, e_2, \dots, e_t\}$ of experiences $e_t = (s_t, a_t, r_t, s_{t+1})$ from many episodes. When training the Q -network, instead only using the current experience as prescribed by standard temporal-difference learning, the network is trained by sampling mini-batches of experiences from \mathcal{D} uniformly at random. The sequence of losses thus takes the form

$$L_i(\theta_i) = \mathbb{E}_{(s,a,r,s') \sim \mathcal{U}(\mathcal{D})} \left[\left(y_i^{DQN} - Q(s, a; \theta_i) \right)^2 \right]. \quad (8)$$

Experience replay increases data efficiency through re-use of experience samples in multiple updates and, importantly, it reduces variance as uniform sampling from the replay buffer reduces the correlation among the samples used in the update.

2.2 DOUBLE DEEP Q-NETWORKS

The previous section described the main components of DQN as presented in (Mnih et al., 2015). In this paper, we use the improved Double DQN (DDQN) learning algorithm of van Hasselt et al. (2015). In Q -learning and DQN, the max operator uses the same values to both select and evaluate an action. This can therefore lead to overoptimistic value estimates (van Hasselt, 2010). To mitigate this problem, DDQN uses the following target:

$$y_i^{DDQN} = r + \gamma Q(s', \arg \max_{a'} Q(s', a'; \theta_i); \theta^-), \quad (9)$$

DDQN is the same as for DQN (see Mnih et al. (2015)), but with the target y_i^{DQN} replaced by y_i^{DDQN} . The pseudo-code for DDQN is presented in Appendix A.

3 THE DUELING NETWORK ARCHITECTURE

The key insight behind our new architecture, as illustrated in Figure 2, is that for many states, it is unnecessary to estimate the value of each action choice. For example, in the Enduro game setting, knowing whether to move left or right only matters when a collision is eminent. In some states, it is of paramount importance to know which action to take, but in many other states the choice of action has no repercussion on what happens. For bootstrapping based algorithms, however, the estimation of state values is of great importance for every state.

To bring this insight to fruition, we must design a network architecture capable of learning the value of a state irrespective of the action choice. In addition, this architecture must also include a component that specifies which actions are preferable in a given state. Last but not least, the new

network must not require the design of new special learning algorithms — it should be able to work with a variety of well-established learning algorithms, such as DQN, double DQN and SARSA.

We accomplish this by considering a decomposition of the Q network into two separate streams: a value stream and an advantage stream, as shown in Figure 1. The input is followed by a number of convolutional and/or pooling layers. Then, the activations of the last of these layers is sent to both separate streams. Each stream contains a number of fully-connected layers. The final layer combines the output of the two streams, and the output of the network is a set of Q values, one for each action. This new Q network can be used with any existing algorithms, such as DQN and Double DQN, without modification. Moreover, this two-stream network can also take advantage of any improvements to these algorithms, including better replay memories, better exploration policies, intrinsic motivation, reward shaping, and so on.

An immediate question is how to design the *aggregator* (i.e., the \oplus module in Figure 1) for combining the value and advantage streams to produce a Q function. Using the definition of advantage function, from equation (4), we have:

$$Q(s, a; \theta, \alpha, \beta) = \widehat{V}(s; \theta, \beta) + \widehat{A}(s, a; \theta, \alpha), \quad (10)$$

where α, β , and θ denote the separate parameters associated with the advantage stream only, value stream only, and remaining parameters, respectively. Note that the expression applies to all (s, a) instances; that is, to express equation (10) in matrix form we need to replicate $\widehat{V}(s; \theta, \beta) |\mathcal{A}|$ times.

The aggregator of equation (10) is unidentifiable in the sense that given Q we cannot recover \widehat{V} and \widehat{A} . To see this, add a constant to \widehat{V} and subtract the same constant from \widehat{A} . This constant cancels out resulting in the same Q value. This lack of identifiability is mirrored by poor practical performance when this equation is used directly.

To remove the extra degree of freedom in equation (10), we propose the following aggregator:

$$Q(s, a; \theta, \alpha, \beta) = \widehat{V}(s; \theta, \beta) + \left(\widehat{A}(s, a; \theta, \alpha) - \frac{1}{|\mathcal{A}|} \sum_{a'} \widehat{A}(s, a'; \theta, \alpha) \right), \quad (11)$$

giving rise to what we call the *dueling network*. Note that while subtracting the mean helps remove this degree of freedom, it does not change the relative rank of the \widehat{A} (and hence Q) values, preserving any greedy or ϵ -greedy policy based on Q values from equation (10). When acting, it suffices to evaluate the advantage stream to make decisions.

It is important to note that equation (11) is viewed and implemented as part of the network and not as a separate algorithmic step. Training of the dueling architectures, as with standard Q networks (e.g. DQN network of Mnih et al. (2015)), requires only back-propagation. The estimates \widehat{V} and \widehat{A} are produced automatically without any extra supervision or algorithmic modifications.

As the dueling architecture shares the same input and output structure with standard Q networks, we can recycle all learning algorithms with Q networks (e.g., DQN, double DQN, SARSA) to train the dueling architecture.

4 EXPERIMENTS

We now show the practical performance of the dueling network. We start with a simple policy evaluation task and then show larger scale results for learning policies for general Atari game-playing.

4.1 POLICY EVALUATION

We start by measuring the performance of the dueling architecture on a policy evaluation task. This task is ideal for evaluating network architectures as it is devoid of confounding factors, such as the choice of exploration strategy, and the interaction between policy improvement and policy evaluation.

In this experiment, we employ temporal difference learning (without eligibility traces, i.e., $\lambda = 0$) to learn Q values. More specifically, given a behavior policy π , we seek to estimate the state-action

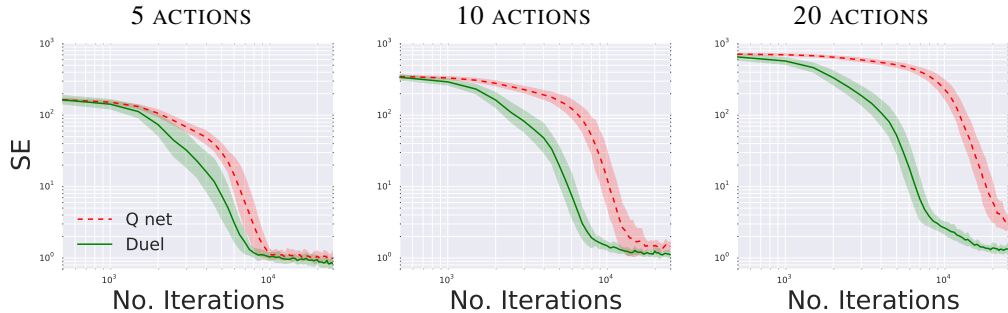


Figure 4: Squared error for policy evaluation with 5, 10, and 20 actions. The dueling network (Duel) consistently outperforms a conventional single-stream convolutional network (Q net), with the performance gap increasing with the number of actions.

value $Q^\pi(\cdot, \cdot)$ by optimizing the sequence of costs of equation (5), with target

$$y_i = r + \gamma \mathbb{E}_{a' \sim \pi(s')} [Q(s', a'; \theta_i)].$$

The above update rule is the same as that of Expected SARSA (van Seijen et al., 2009). We, however, do not modify the behavior policy as in Expected SARSA.

To evaluate the learned Q values, we choose a simple environment where the exact $Q^\pi(s, a)$ values can be computed separately for all $(s, a) \in \mathcal{S} \times \mathcal{A}$. This environment, which we call the *corridor* is composed of three connected corridors. A schematic drawing of the corridor environment is shown in Figure 3. The agent starts from the bottom left corner of the environment and must move to the top right to get the largest reward. A total of 5 actions are available: go up, down, left, right and no-op. We also have the freedom of adding an arbitrary number of no-op actions. In our setup, the two vertical sections both have 10 states while the horizontal section has 50.

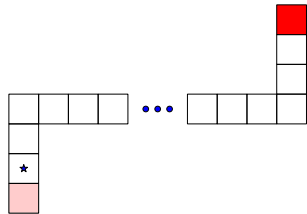


Figure 3: The corridor environment. The star marks the starting state. The redness of a state signifies the reward the agent receives upon arrival. The game terminates upon reaching either reward state. The agent’s actions are going up, down, left, right and no action.

We use an ϵ -greedy policy as the behavior policy π , which chooses a random action with probability ϵ or an action according to the optimal Q function $\arg \max_{a \in \mathcal{A}} Q^*(s, a)$ with probability $1 - \epsilon$. In our experiments, ϵ is chosen to be 0.001.

We compare a single-stream Q architecture with the dueling architecture on three variants of the corridor environment with 5, 10 and 20 actions respectively.

The 10 and 20 action variants are formed by adding no-ops to the original environment. We measure performance by Squared Error (SE) against the true state values: $\sum_{s \in \mathcal{S}, a \in \mathcal{A}} (Q(s, a; \theta) - Q^\pi(s, a))^2$. The single-stream architecture is a three layer MLP with 50 units on each hidden layer. The dueling architecture is also composed of three layers. After the first hidden layer of 50 units, however, the network branches off into two streams each of them a two layer MLP with 25 hidden units. The results of the comparison are summarized in Figure 4.

With 5 actions, both architectures converge at about the same speed. But as we increase the number of actions, we can see that the dueling architecture performs better relative to the traditional Q -network. The stream $\widehat{V}(s; \theta, \beta)$ learns a general value that is shared across many similar actions at s . This is important as many control tasks with large action spaces manifest this property.

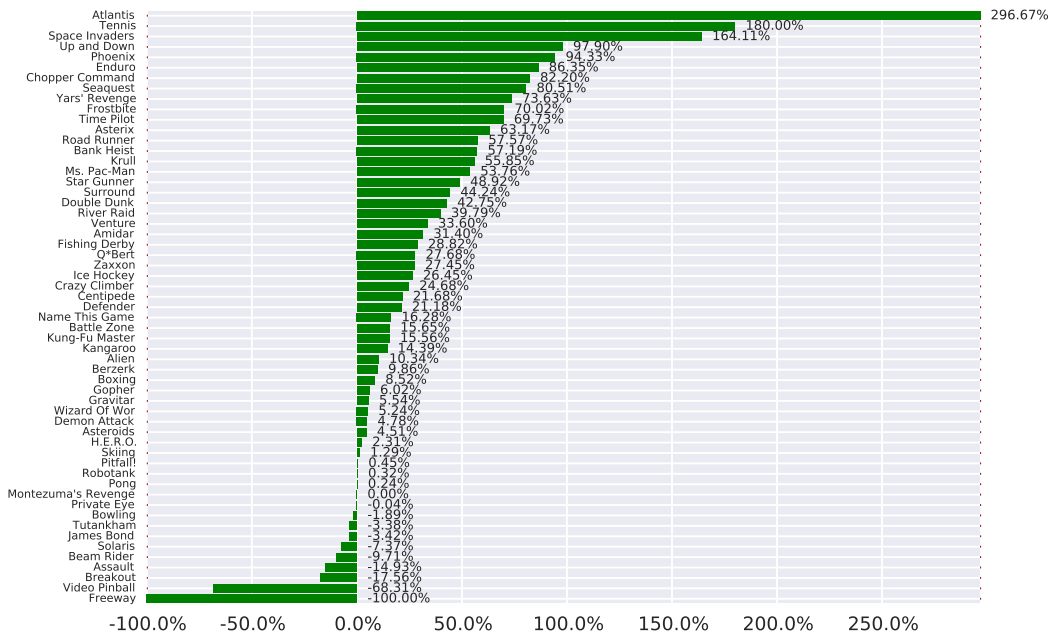


Figure 5: Comparison to Double DQN using the metric described in Equation (12). A bar to the right indicates the percentage by means of which the dueling agent outperforms DDQN.

4.2 GENERAL ATARI GAME-PLAYING

We perform a comprehensive evaluation of our proposed method on the Arcade Learning Environment (Bellemare et al., 2013), which is composed of 57 Atari games. The challenge is to deploy a single algorithm and architecture, with a fixed set of hyper-parameters, to learn to play all the games given only raw pixel observations and game rewards. This environment is very demanding because it is both comprised of a large number of highly diverse games and the observations are high-dimensional.

We follow closely the setup of van Hasselt et al. (2015) and compare to their results. Importantly, we adopt the DDQN algorithm as presented in Appendix A. Our network architecture has the same low-level convolutional structure of DQN (Mnih et al., 2015; van Hasselt et al., 2015), but it incorporates the dueling streams described in Section 3 after the convolutional layers. We duplicate the fully-connected layers of DQN to construct the dueling architecture streams. In more detail, there are three convolutional layers followed by 2 fully-connected layers. The first convolutional layer has $32 \times 8 \times 8$ filters with stride 4, the second $64 \times 4 \times 4$ filters with stride 2, and the third and final convolutional layer consists $64 \times 3 \times 3$ filters with stride 1. As depicted in Figure 1, the network diverges into two streams after the convolutional layers, with one stream computing \hat{V} and the other \hat{A} . The value and advantage streams both have a fully-connected layer with 512 units. The final hidden layers of the value and advantage streams are both fully-connected with the value stream having one output and the advantage as many outputs as there are valid actions². Rectifier non-linearities (Fukushima, 1980) are inserted between all adjacent layers.

We adopt the optimizers and hyper-parameters of van Hasselt et al. (2015), with the exception of the learning rate which we chose to be slightly lower (we do not do this for double DQN as it can deteriorate its performance). In addition, we clip the gradients to have their norm less than or equal to 10. This clipping is not standard practice in deep RL, but a common in recurrent network training (Bengio et al., 2013). Since both the advantage and the value stream propagate gradients to the last convolutional layer in the backward pass, we rescale the combined gradient entering the last convolutional layer by $1/\sqrt{2}$. This simple heuristic mildly increases stability.

²The number of actions ranges between 4-18 actions in the ALE environment.

Table 1: Mean and median scores measured in human performance for the 57 Atari games.

	30 no-ops		Human Starts	
	Mean	Median	Mean	Median
Duel	373.1%	151.5%	343.8%	117.1%
DDQN	307.3%	117.8%	332.9%	110.9%
DQN	227.9%	79.1%	219.6%	68.5%

As in (van Hasselt et al., 2015), we start the game with up to 30 no-op actions to provide random starting positions for the agent. To evaluate our approach, we measure improvement in percentage (positive or negative) in score over the better of human and DDQN scores:

$$\text{Improvement} = \frac{\text{Score}_{\text{Agent}} - \text{Score}_{\text{Random}}}{\max\{\text{Score}_{\text{Human}}, \text{Score}_{\text{DDQN}}\} - \text{Score}_{\text{Random}}}. \quad (12)$$

We took the maximum over human and DDQN scores as it prevents insignificant changes to appear as large improvements when neither the agent in question nor DDQN are doing well. For example, an agent that achieves 2% human performance should not be interpreted as two times better when DDQN achieves 1% human performance. We also chose not to measure performance in terms of percentage of human performance alone because a tiny difference relative to DDQN on some games can translate into hundreds of percent in human performance difference.

The resulting comparison is presented in Figure 5. The mean and median performance against the human performance percentage is shown in Table 1³.

Our approach achieves higher scores compared to the baseline on 80.7% (46 out of 57) of the games. Of all the games with 18 actions, the dueling architecture is better 86.6% of the time (26 out of 30). This is consistent with the findings of the previous section. Overall, our agent achieves human level performance on 42 out of 57 games. Raw scores for all the games, as well as measurements in human performance percentage, are presented in Appendix B.

To isolate the contributions of the dueling architecture, we re-train DDQN using exactly the same procedure as the one used to train the dueling architecture. Notably, we apply gradient clipping to DDQN, and use 1024 hidden units for the first fully-connected layer of the network in DDQN so that both architectures have roughly the same number of parameters.

The dueling architecture does equally or better than the gradient-clipped DDQN on 75.4% of the games (43 out of 57). The gradient-clipped DDQN achieves mean and median scores of 341.2% and 132.6% respectively on the 30 no-ops performance measure. These scores are markedly lower than the scores of the dueling architecture. Despite the gains brought in by gradient clipping, the dueling architecture still maintains a significant edge over traditional architectures of similar complexity (number of parameters).

A few training curves, shown in Figure 6, compare the dueling architecture, and DDQN with the traditional Q architecture with and without gradient clipping.

Robustness to human starts. One shortcoming of the previous metric is that an agent does not necessarily have to generalize well to play the Atari games. Due to the deterministic nature of the Atari environment, from a unique starting point, an agent could learn to achieve good performance by simply remembering sequences of actions.

To obtain a more robust measure, we adopt the methodology of Nair et al. (2015). Specifically, for each game, we use 100 starting points sampled from a human expert’s trajectory. From each of these points, an evaluation episode is launched for up to 108,000 frames. The agents are evaluated only on rewards accrued after the starting point.

³ When calculating the human performance percentage for the game Video Pinball, the random scores are set to zero. This is because human scores on this game are lower than that of a random agent making the calculation of human performance percentage invalid. Resetting the random score does not affect the median scores of the agents considered. The mean scores, however, are affected.

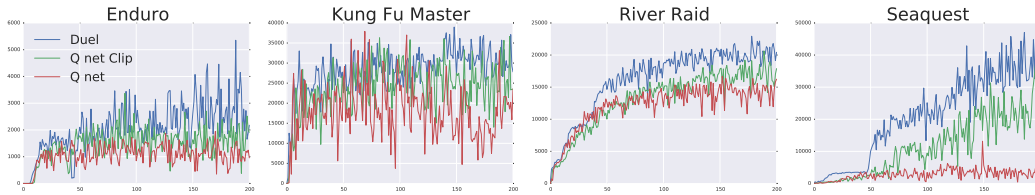


Figure 6: Performance evaluated at training time on four Atari games. The curves correspond to three instances of the DDQN algorithm using a convolutional network of similar size to the dueling network (Q net) using the same convolutional network and gradient clipping (Q net Clip) and using the dueling network (Duel).

With this measure, the dueling agent does better than the baseline on 70.2% (40 out of 57) games and on games of 18 actions, the dueling agent is 83.3% better (25 out of 30). The comparison to the baseline in human performance percentage is presented in Table 1.

Saliency maps. To better understand the roles of the value and the advantage streams, we compute saliency maps (Simonyan et al., 2013). More specifically, to visualize the salient part of the image as seen by the value stream, we compute the absolute value of the Jacobian of \hat{V} with respect to the input frames: $|\nabla_s \hat{V}(s; \theta)|$. Similarly, to visualize the salient part of the image as seen by the advantage stream, we compute $|\nabla_s \hat{A}(s, \arg \max_{a'} \hat{A}(s, a'); \theta)|$. Both quantities are of the same dimensionality as the input frames and therefore can be visualized easily alongside the input frames.

Here, we place the gray scale input frames in the green and blue channel and the saliency maps in the red channel. All three channels together form an RGB image. Figure 2 depicts the value and advantage saliency maps on the Enduro game for two different time steps. As observed in the introduction, the value stream pays attention to the horizon where the appearance of a car could affect future performance. The value stream also pays attention to the score. The advantage stream, on the other hand, cares more about cars that are on an immediate collision course.

5 DISCUSSION

The advantages of the dueling architecture lie partly in its ability to learn the state-value function efficiently. With every update of the Q values in the dueling architecture, the value stream \hat{V} is updated. Since the value stream forms a good approximation of the state value when the variation of Q values between actions is small, this frequent updating of the value stream allows for better approximation of the state values.

The variation of state action values for a given state is indeed often very small. For example, after training with DDQN on the game of Seaquest, the average action gap (the gap between the Q values of the best and the second best action in a given state) across visited states is roughly 0.04. In comparison, the average state value across visited states is about 15.

With small variations between actions, bootstrapping (Sutton & Barto, 1998) depends heavily on the state values. Accurate estimation of state values thus enables the dueling architecture to be more effective in bootstrapping-based approaches.

As demonstrated in the experiments, the advantage of the dueling architecture over standard Q networks is especially prominent when the number of actions is large. With more actions, the estimate of state values becomes difficult in standard Q networks even with small variations between actions. For example, with the variation between actions being small, the Q network effectively has to learn the same value for all actions while each update only modifies the Q value of one action. The dueling architecture, on the other hand, maintains its ability to estimate the state values regardless of the number of actions.

6 CONCLUSIONS

We introduced a new neural network architecture that decouples value and advantage in deep Q -networks, while sharing a common feature learning module. The new architecture, in combination with some algorithmic improvements, leads to dramatic improvements over existing approaches for deep RL in the challenging Atari domain. The new architecture was also shown to provide performance increases in policy evaluation. We also found out that gradient clipping is very effective in this domain and recommend its usage to the deep RL community.

Since most recent advances in deep RL have been the result of algorithmic improvements (and not architecture improvements) (van Hasselt et al., 2015; Bellemare et al., 2016; Schaul et al., 2015), we believe our dueling architecture could lead to further improvements when combined with these new algorithms. Of particular promise is the combination of the dueling architecture with prioritized replay.

ACKNOWLEDGMENTS

We would like to thank Hado van Hasselt, Arthur Guez, Vlad Mnih, Nicolas Hess, Marc Bellemare, Georg Ostrovski, Tom Schaul and all the folks at Google DeepMind for making this possible.

REFERENCES

- Ba, J., Mnih, V., and Kavukcuoglu, K. Multiple object recognition with visual attention. In *ICLR*, 2015.
- Baird, L.C. Advantage updating. Technical Report WL-TR-93-1146, Wright-Patterson Air Force Base, 1993.
- Bellemare, M. G., Naddaf, Y., Veness, J., and Bowling, M. The arcade learning environment: An evaluation platform for general agents. *Journal of Artificial Intelligence Research*, 47:253–279, 2013.
- Bellemare, M. G., Ostrovski, G., Guez, A., Thomas, P. S., and Munos, R. Increasing the action gap: New operators for reinforcement learning. In *AAAI*, 2016. To appear.
- Bengio, Y., Boulanger-Lewandowski, N., and Pascanu, R. Advances in optimizing recurrent networks. In *ICASSP*, pp. 8624–8628, 2013.
- Fukushima, K. Neocognitron: A self-organizing neural network model for a mechanism of pattern recognition unaffected by shift in position. *Biological Cybernetics*, 36:193–202, 1980.
- Guo, X., Singh, S., Lee, H., Lewis, R. L., and Wang, X. Deep learning for real-time Atari game play using offline Monte-Carlo tree search planning. In *NIPS*, pp. 3338–3346. 2014.
- Harmon, M.E. and Baird, L.C. Multi-player residual advantage learning with general function approximation. Technical Report WL-TR-1065, Wright-Patterson Air Force Base, 1996.
- Harmon, M.E., Baird, L.C., and Klopff, A.H. Advantage updating applied to a differential game. In G. Tesauro, D.S. Touretzky and Leen, T.K. (eds.), *NIPS*, 1995.
- LeCun, Y., Bengio, Y., and Hinton, G. Deep learning. *Nature*, 521(7553):436–444, 2015.
- Levine, S., Finn, C., Darrell, T., and Abbeel, P. End-to-end training of deep visuomotor policies. *arXiv preprint arXiv:1504.00702*, 2015.
- Lin, L.J. *Reinforcement learning for robots using neural networks*. PhD thesis, School of Computer Science, Carnegie Mellon University, 1993.
- Maddison, C. J., Huang, A., Sutskever, I., and Silver, D. Move Evaluation in Go Using Deep Convolutional Neural Networks. In *ICLR*, 2015.

- Mnih, V., Kavukcuoglu, K., Silver, D., Rusu, A. A., Veness, J., Bellemare, M. G., Graves, A., Riedmiller, M., Fidjeland, A. K., Ostrovski, G., Petersen, S., Beattie, C., Sadik, A., Antonoglou, I., King, H., Kumaran, D., Wierstra, D., Legg, S., and Hassabis, D. Human-level control through deep reinforcement learning. *Nature*, 518(7540):529–533, 2015.
- Nair, A., Srinivasan, P., Blackwell, S., Alcicek, C., Fearon, R., Maria, A. De, Panneershelvam, V., Suleyman, M., Beattie, C., Petersen, S., Legg, S., Mnih, V., Kavukcuoglu, K., and Silver, D. Massively parallel methods for deep reinforcement learning. In *Deep Learning Workshop, ICML*, 2015.
- Schaul, T., Quan, J., Antonoglou, I., and Silver, D. Prioritized experience replay. Technical report, 2015.
- Schulman, J., Moritz, P., Levine, S., Jordan, M. I., and Abbeel, P. High-dimensional continuous control using generalized advantage estimation. *arXiv preprint arXiv:1506.02438*, 2015.
- Simonyan, K., Vedaldi, A., and Zisserman, A. Deep inside convolutional networks: Visualising image classification models and saliency maps. *arXiv preprint arXiv:1312.6034*, 2013.
- Stadie, B. C., Levine, S., and Abbeel, P. Incentivizing exploration in reinforcement learning with deep predictive models. *arXiv preprint arXiv:1507.00814*, 2015.
- Sutton, R. S. and Barto, A. G. *Introduction to reinforcement learning*. MIT Press, 1998.
- Sutton, R. S., Mcallester, D., Singh, S., and Mansour, Y. Policy gradient methods for reinforcement learning with function approximation. In *NIPS*, pp. 1057–1063, 2000.
- van Hasselt, H. Double Q-learning. *NIPS*, 23:2613–2621, 2010.
- van Hasselt, H., Guez, A., and Silver, D. Deep reinforcement learning with double Q-learning. *arXiv preprint arXiv:1509.06461*, 2015.
- van Seijen, H., van Hasselt, H., Whiteson, S., and Wiering, M. A theoretical and empirical analysis of Expected Sarsa. In *IEEE Symposium on Adaptive Dynamic Programming and Reinforcement Learning*, pp. 177–184. 2009.
- Watter, M., Springenberg, J. T., Boedecker, J., and Riedmiller, M. A. Embed to control: A locally linear latent dynamics model for control from raw images. In *NIPS*, 2015.

A DOUBLE DEEP Q-NETWORK LEARNING ALGORITHM

Algorithm 1: Double Deep Q-networks (DDQN) Algorithm.

input : \mathcal{D} – empty replay buffer; θ – initial network parameters, θ^- – copy of θ
input : N_r – replay buffer maximum size; N_b – training batch size; N^- – target network replacement freq.
for episode $e \in \{1, 2, \dots, M\}$ **do**
 Initialize frame sequence $\mathbf{x} \leftarrow ()$
 for $t \in \{0, 1, \dots\}$ **do**
 Set state $s \leftarrow \mathbf{x}$, sample action from behavior policy $a \sim \pi_B$
 Sample next frame x^t from environment \mathcal{E} given (s, a) and receive reward r , and append x^t to \mathbf{x}
 if $|\mathbf{x}| > N_f$ **then** delete the oldest frame $x_{t_{min}}$ from \mathbf{x} **end**
 Set $s' \leftarrow \mathbf{x}$, and add transition tuple (s, a, r, s') to \mathcal{D} , replacing the oldest tuple if $|\mathcal{D}| \geq N_r$
 Sample a minibatch of N_b tuples (s, a, r, s') uniformly from \mathcal{D}
 Construct target values, one for each of the N_b tuples:

$$y_j = \begin{cases} r & \text{if } s' \text{ is terminal} \\ r + \gamma Q(s', \arg \max_{a'} Q(s', a'; \theta); \theta^-), & \text{otherwise.} \end{cases}$$

 Perform a gradient descent step on loss $\|y_j - Q(s, a; \theta)\|^2$
 Replace target network parameters $\theta^- \leftarrow \theta$ every N^- steps
 end
end

B SCORE TABLES

Table 2: Raw scores across all games. Starting with **30 no-op** actions.

Games	No. Actions	Random	Human	DQN	DDQN	Duel
Alien	18	227.8	7,127.7	1,620.0	3,747.7	4,461.4
Amidar	10	5.8	1,719.5	978.0	1,793.3	2,354.5
Assault	7	222.4	742.0	4,280.4	5,393.2	4,621.0
Asterix	9	210.0	8,503.3	4,359.0	17,356.5	28,188.0
Asteroids	14	719.1	47,388.7	1,364.5	734.7	2,837.7
Atlantis	4	12,850.0	29,028.1	279,987.0	106,056.0	382,572.0
Bank Heist	18	14.2	753.1	455.0	1,030.6	1,611.9
Battle Zone	18	2,360.0	37,187.5	29,900.0	31,700.0	37,150.0
Beam Rider	9	363.9	16,926.5	8,627.5	13,772.8	12,164.0
Berzerk	18	123.7	2,630.4	585.6	1,225.4	1,472.6
Bowling	6	23.1	160.7	50.4	68.1	65.5
Boxing	18	0.1	12.1	88.0	91.6	99.4
Breakout	4	1.7	30.5	385.5	418.5	345.3
Centipede	18	2,090.9	12,017.0	4,657.7	5,409.4	7,561.4
Chopper Command	18	811.0	7,387.8	6,126.0	5,809.0	11,215.0
Crazy Climber	9	10,780.5	35,829.4	110,763.0	117,282.0	143,570.0
Defender	18	2,874.5	18,688.9	23,633.0	35,338.5	42,214.0
Demon Attack	6	152.1	1,971.0	12,149.4	58,044.2	60,813.3
Double Dunk	18	-18.6	-16.4	-6.6	-5.5	0.1
Enduro	9	0.0	860.5	729.0	1,211.8	2,258.2
Fishing Derby	18	-91.7	-38.7	-4.9	15.5	46.4
Freeway	3	0.0	29.6	30.8	33.3	0.0
Frostbite	18	65.2	4,334.7	797.4	1,683.3	4,672.8
Gopher	8	257.6	2,412.5	8,777.4	14,840.8	15,718.4
Gravitar	18	173.0	3,351.4	473.0	412.0	588.0
H.E.R.O.	18	1,027.0	30,826.4	20,437.8	20,130.2	20,818.2
Ice Hockey	18	-11.2	0.9	-1.9	-2.7	0.5
James Bond	18	29.0	302.8	768.5	1,358.0	1,312.5
Kangaroo	18	52.0	3,035.0	7,259.0	12,992.0	14,854.0
Krull	18	1,598.0	2,665.5	8,422.3	7,920.5	11,451.9
Kung-Fu Master	14	258.5	22,736.3	26,059.0	29,710.0	34,294.0
Montezuma's Revenge	18	0.0	4,753.3	0.0	0.0	0.0
Ms. Pac-Man	9	307.3	6,951.6	3,085.6	2,711.4	6,283.5
Name This Game	6	2,292.3	8,049.0	8,207.8	10,616.0	11,971.1
Phoenix	8	761.4	7,242.6	8,485.2	12,252.5	23,092.2
Pitfall!	18	-229.4	6,463.7	-286.1	-29.9	0.0
Pong	3	-20.7	14.6	19.5	20.9	21.0
Private Eye	18	24.9	69,571.3	146.7	129.7	103.0
Q*Bert	6	163.9	13,455.0	13,117.3	15,088.5	19,220.3
River Raid	18	1,338.5	17,118.0	7,377.6	14,884.5	21,162.6
Road Runner	18	11.5	7,845.0	39,544.0	44,127.0	69,524.0
Robotank	18	2.2	11.9	63.9	65.1	65.3
Seaquest	18	68.4	42,054.7	5,860.6	16,452.7	50,254.2
Skiing	3	-17,098.1	-4,336.9	-13,062.3	-9,021.8	-8,857.4
Solaris	18	1,236.3	12,326.7	3,482.8	3,067.8	2,250.8
Space Invaders	6	148.0	1,668.7	1,692.3	2,525.5	6,427.3
Star Gunner	18	664.0	10,250.0	54,282.0	60,142.0	89,238.0
Surround	5	-10.0	6.5	-5.6	-2.9	4.4
Tennis	18	-23.8	-8.3	12.2	-22.8	5.1
Time Pilot	10	3,568.0	5,229.2	4,870.0	8,339.0	11,666.0
Tutankham	8	11.4	167.6	68.1	218.4	211.4
Up and Down	6	533.4	11,693.2	9,989.9	22,972.2	44,939.6
Venture	18	0.0	1,187.5	163.0	98.0	497.0
Video Pinball	9	16,256.9	17,667.9	196,760.4	309,941.9	98,209.5
Wizard Of Wor	10	563.5	4,756.5	2,704.0	7,492.0	7,855.0
Yars' Revenge	18	3,092.9	54,576.9	18,098.9	11,712.6	49,622.1
Zaxxon	18	32.5	9,173.3	5,363.0	10,163.0	12,944.0

Table 3: Raw scores across all games. Starting with **Human starts**.

Games	No. Actions	Random	Human	DQN	DDQN	Duel
Alien	18	128.3	6,371.3	634.0	1,033.4	1,486.5
Amidar	10	11.8	1,540.4	178.4	169.1	172.7
Assault	7	166.9	628.9	3,489.3	6,060.8	3,994.8
Asterix	9	164.5	7,536.0	3,170.5	16,837.0	15,840.0
Asteroids	14	871.3	36,517.3	1,458.7	1,193.2	2,035.4
Atlantis	4	13,463.0	26,575.0	292,491.0	319,688.0	445,360.0
Bank Heist	18	21.7	644.5	312.7	886.0	1,129.3
Battle Zone	18	3,560.0	33,030.0	23,750.0	24,740.0	31,320.0
Beam Rider	9	254.6	14,961.0	9,743.2	17,417.2	14,591.3
Berzerk	18	196.1	2,237.5	493.4	1,011.1	910.6
Bowling	6	35.2	146.5	56.5	69.6	65.7
Boxing	18	-1.5	9.6	70.3	73.5	77.3
Breakout	4	1.6	27.9	354.5	368.9	411.6
Centipede	18	1,925.5	10,321.9	3,973.9	3,853.5	4,881.0
Chopper Command	18	644.0	8,930.0	5,017.0	3,495.0	3,784.0
Crazy Climber	9	9,337.0	32,667.0	98,128.0	113,782.0	124,566.0
Defender	18	1,965.5	14,296.0	15,917.5	27,510.0	33,996.0
Demon Attack	6	208.3	3,442.8	12,550.7	69,803.4	56,322.8
Double Dunk	18	-16.0	-14.4	-6.0	-0.3	-0.8
Enduro	9	-81.8	740.2	626.7	1,216.6	2,077.4
Fishing Derby	18	-77.1	5.1	-1.6	3.2	-4.1
Freeway	3	0.1	25.6	26.9	28.8	0.2
Frostbite	18	66.4	4,202.8	496.1	1,448.1	2,332.4
Gopher	8	250.0	2,311.0	8,190.4	15,253.0	20,051.4
Gravitar	18	245.5	3,116.0	298.0	200.5	297.0
H.E.R.O.	18	1,580.3	25,839.4	14,992.9	14,892.5	15,207.9
Ice Hockey	18	-9.7	0.5	-1.6	-2.5	-1.3
James Bond	18	33.5	368.5	697.5	573.0	835.5
Kangaroo	18	100.0	2,739.0	4,496.0	11,204.0	10,334.0
Krull	18	1,151.9	2,109.1	6,206.0	6,796.1	8,051.6
Kung-Fu Master	14	304.0	20,786.8	20,882.0	30,207.0	24,288.0
Montezuma's Revenge	18	25.0	4,182.0	47.0	42.0	22.0
Ms. Pac-Man	9	197.8	15,375.0	1,092.3	1,241.3	2,250.6
Name This Game	6	1,747.8	6,796.0	6,738.8	8,960.3	11,185.1
Phoenix	8	1,134.4	6,686.2	7,484.8	12,366.5	20,410.5
Pitfall!	18	-348.8	5,998.9	-113.2	-186.7	-46.9
Pong	3	-18.0	15.5	18.0	19.1	18.8
Private Eye	18	662.8	64,169.1	207.9	-575.5	292.6
Q*Bert	6	183.0	12,085.0	9,271.5	11,020.8	14,175.8
River Raid	18	588.3	14,382.2	4,748.5	10,838.4	16,569.4
Road Runner	18	200.0	6,878.0	35,215.0	43,156.0	58,549.0
Robotank	18	2.4	8.9	58.7	59.1	62.0
Seaquest	18	215.5	40,425.8	4,216.7	14,498.0	37,361.6
Skiing	3	-15,287.4	-3,686.6	-12,142.1	-11,490.4	-11,928.0
Solaris	18	2,047.2	11,032.6	1,295.4	810.0	1,768.4
Space Invaders	6	182.6	1,464.9	1,293.8	2,628.7	5,993.1
Star Gunner	18	697.0	9,528.0	52,970.0	58,365.0	90,804.0
Surround	5	-9.7	5.4	-6.0	1.9	4.0
Tennis	18	-21.4	-6.7	11.1	-7.8	4.4
Time Pilot	10	3,273.0	5,650.0	4,786.0	6,608.0	6,601.0
Tutankham	8	12.7	138.3	45.6	92.2	48.0
Up and Down	6	707.2	9,896.1	8,038.5	19,086.9	24,759.2
Venture	18	18.0	1,039.0	136.0	21.0	200.0
Video Pinball	9	20452.0	15,641.1	154,414.1	367,823.7	110,976.2
Wizard Of Wor	10	804.0	4,556.0	1,609.0	6,201.0	7,054.0
Yars' Revenge	18	1,476.9	47,135.2	4,577.5	6,270.6	25,976.5
Zaxxon	18	475.0	8,443.0	4,412.0	8,593.0	10,164.0

Table 4: Normalized scores across all games. Starting with **30 no-op** actions.

Games	DQN	DDQN	Duel
Alien	20.2%	51.0%	61.4%
Amidar	56.7%	104.3%	137.1%
Assault	781.0%	995.1%	846.5%
Asterix	50.0%	206.8%	337.4%
Asteroids	1.4%	0.0%	4.5%
Atlantis	1651.2%	576.1%	2285.3%
Bank Heist	59.7%	137.6%	216.2%
Battle Zone	79.1%	84.2%	99.9%
Beam Rider	49.9%	81.0%	71.2%
Berzerk	18.4%	44.0%	53.8%
Bowling	19.8%	32.7%	30.8%
Boxing	732.5%	762.1%	827.1%
Breakout	1334.5%	1449.2%	1194.5%
Centipede	25.9%	33.4%	55.1%
Chopper Command	80.8%	76.0%	158.2%
Crazy Climber	399.1%	425.2%	530.1%
Defender	131.3%	205.3%	248.8%
Demon Attack	659.6%	3182.8%	3335.0%
Double Dunk	557.7%	607.9%	866.5%
Enduro	84.7%	140.8%	262.4%
Fishing Derby	163.8%	202.4%	260.7%
Freeway	104.0%	112.5%	0.1%
Frostbite	17.1%	37.9%	107.9%
Gopher	395.4%	676.7%	717.5%
Gravitar	9.4%	7.5%	13.1%
H.E.R.O.	65.1%	64.1%	66.4%
Ice Hockey	76.9%	70.0%	96.4%
James Bond	270.1%	485.4%	468.8%
Kangaroo	241.6%	433.8%	496.2%
Krull	639.3%	592.3%	923.1%
Kung-Fu Master	114.8%	131.0%	151.4%
Montezuma's Revenge	0.0%	0.0%	0.0%
Ms. Pac-Man	41.8%	36.2%	89.9%
Name This Game	102.8%	144.6%	168.1%
Phoenix	119.2%	177.3%	344.5%
Pitfall!	-0.8%	3.0%	3.4%
Pong	114.0%	117.8%	118.2%
Private Eye	0.2%	0.2%	0.1%
Q*Bert	97.5%	112.3%	143.4%
River Raid	38.3%	85.8%	125.6%
Road Runner	504.7%	563.2%	887.4%
Robotank	631.5%	643.7%	645.1%
Seaquest	13.8%	39.0%	119.5%
Skiing	31.6%	63.3%	64.6%
Solaris	20.3%	16.5%	9.1%
Space Invaders	101.6%	156.3%	412.9%
Star Gunner	559.3%	620.5%	924.0%
Surround	26.5%	43.2%	86.9%
Tennis	231.3%	6.8%	186.2%
Time Pilot	78.4%	287.2%	487.5%
Tutankham	36.3%	132.5%	128.1%
Up and Down	84.7%	201.1%	397.9%
Venture	13.7%	8.3%	41.9%
Video Pinball	1113.7%	1754.3%	555.9%
Wizard Of Wor	51.0%	165.2%	173.9%
Yars' Revenge	29.1%	16.7%	90.4%
Zaxxon	58.3%	110.8%	141.3%
Mean	227.9%	307.3%	373.1%
Median	79.1%	117.8%	151.4%

Table 5: Normalized scores across all games. Starting with **Human Starts**.

Games	DQN	DDQN	Duel
Alien	8.1%	14.5%	21.8%
Amidar	10.9%	10.3%	10.5%
Assault	719.2%	1275.9%	828.6%
Asterix	40.8%	226.2%	212.7%
Asteroids	1.6%	0.9%	3.3%
Atlantis	2128.0%	2335.5%	3293.9%
Bank Heist	46.7%	138.8%	177.8%
Battle Zone	68.5%	71.9%	94.2%
Beam Rider	64.5%	116.7%	97.5%
Berzerk	14.6%	39.9%	35.0%
Bowling	19.2%	30.9%	27.5%
Boxing	648.2%	677.0%	711.2%
Breakout	1341.9%	1396.7%	1559.0%
Centipede	24.4%	23.0%	35.2%
Chopper Command	52.8%	34.4%	37.9%
Crazy Climber	380.6%	447.7%	493.9%
Defender	113.2%	207.2%	259.8%
Demon Attack	381.6%	2151.6%	1734.8%
Double Dunk	622.5%	982.5%	948.7%
Enduro	86.2%	158.0%	262.7%
Fishing Derby	91.8%	97.7%	88.8%
Freeway	105.1%	112.5%	0.6%
Frostbite	10.4%	33.4%	54.8%
Gopher	385.3%	727.9%	960.8%
Gravitar	1.8%	-1.6%	1.8%
H.E.R.O.	55.3%	54.9%	56.2%
Ice Hockey	79.2%	70.8%	82.4%
James Bond	198.2%	161.0%	239.4%
Kangaroo	166.6%	420.8%	387.8%
Krull	528.0%	589.7%	720.8%
Kung-Fu Master	100.5%	146.0%	117.1%
Montezuma's Revenge	0.5%	0.4%	-0.1%
Ms. Pac-Man	5.9%	6.9%	13.5%
Name This Game	98.9%	142.9%	186.9%
Phoenix	114.4%	202.3%	347.2%
Pitfall!	3.7%	2.6%	4.8%
Pong	107.6%	110.9%	110.0%
Private Eye	-0.7%	-1.9%	-0.6%
Q*Bert	76.4%	91.1%	117.6%
River Raid	30.2%	74.3%	115.9%
Road Runner	524.3%	643.2%	873.7%
Robotank	863.3%	868.7%	913.3%
Seaquest	10.0%	35.5%	92.4%
Skiing	27.1%	32.7%	29.0%
Solaris	-8.4%	-13.8%	-3.1%
Space Invaders	86.7%	190.8%	453.1%
Star Gunner	591.9%	653.0%	1020.3%
Surround	24.7%	76.9%	91.1%
Tennis	220.8%	92.1%	175.0%
Time Pilot	63.7%	140.3%	140.0%
Tutankham	26.2%	63.3%	28.1%
Up and Down	79.8%	200.0%	261.8%
Venture	11.6%	0.3%	17.8%
Video Pinball	987.2%	2351.6%	709.5%
Wizard Of Wor	21.5%	143.8%	166.6%
Yars' Revenge	6.8%	10.5%	53.7%
Zaxxon	49.4%	101.9%	121.6%
Mean	219.6%	332.9%	343.8%
Median	68.5%	110.9%	117.1%